European Journal of Pharmaceutics and Biopharmaceutics 139 (2019) 213–223

Contents lists available at ScienceDirect

European Journal of Pharmaceutics and Biopharmaceutics

journal homepage: www.elsevier.com/locate/ejpb

Research paper

Effect of particle deposition density of dry powders on the results produced by an *in vitro* test system simulating dissolution- and absorption rates in the lungs

Maria Malmlöf[a,b,*], Mattias Nowenwik[a], Kristof Meelich[c], Iwona Rådberg[a,1], Ewa Selg[a], John Burns[d], Hermann Mascher[c], Per Gerde[a,b]

[a] *Inhalation Sciences, Stockholm, Sweden*
[b] *Institute of Environmental Medicine, Karolinska Institutet, Stockholm, Sweden*
[c] *Pharm-analyt Labor GmbH, Baden, Austria*
[d] *Circassia, London, United Kingdom*

ARTICLE INFO

Keywords:
DissolvIt
In vitro lung dissolution
Deposition density
PreciseInhale
Inhalation exposure
In vitro *in vivo* correlation

ABSTRACT

The surface area of the air/liquid interface in the lungs is substantial, so deposited doses of aerosol medicines per interface surface area when administered via the inhalation route is always quite low. However, in most *in vitro* systems used for dissolution testing of dry powder inhalables, the dose per surface area is generally much higher.

The aim of this study was to investigate in one *in vitro* lung dissolution system, the DissolvIt, the manner in which the deposited dose per test surface area of drug particles influences the simulated dissolution- and absorption rate.

Here we used the dissolution test method DissolvIt to investigate the influence on dissolution behavior by varying the deposited surface density of tested drugs. Dry powders of three different active pharmaceutical ingredients with different solubilities were used; salmeterol, budesonide and fluticasone propionate.

It was found that by varying the dose density from 0.23 to 29 μg/cm^2 the dissolution- and absorption rate of test particles was affected for all three substances, with decreasing relative dissolution rates above certain dose limits. The effect was much more prominent with the least soluble fluticasone propionate. In contrast, in a real lung it has been shown that a tenfold increase of the even less soluble fluticasone furoate did not affect the pulmonary dissolution- and absorption as measured in the *ex vivo* isolated perfused rat lung.

This indicates that the deposited particle dose on the test surface used must be carefully considered in all *in vitro* dissolution testing apparatuses used for inhalation drugs, especially when aiming for *in vitro-in vivo* correlations. Conclusive data show that in the DissolvIt system consistent normalized dissolution- and absorption data can be obtained if the deposition density of test substance are kept below 1 μg/cm^2 and the variability between the initial drug doses is smaller than 10–15% expressed as standard deviation.

1. Introduction

There is an explicit need within inhalation research for *in vitro* test methods that can better predict *in vivo* responses. One specific need is that *in vitro* data generated for a particulate drug substance can better indicate the clinical pharmacokinetic (PK) outcome following lung deposition such as dissolution, absorption and distribution [1–3]. Such a method would in the future both reduce, refine and replace animal experiments as well as reduce costs in the drug development process, by earlier being able to eliminate failure candidates.

One approach in improving *in vitro* methods is to better mimic the physiological situation in the lung. Following inhalation, the dry powder particles are deposited within the airways. Because the internal surface area of the lungs is quite large, on average 70 m^2 in humans [4], this implies that the effective deposited dose from a dry powder drug of alleged 100 μg, will correspond to an average particle concentration of 1.4 μg/m^2 (= 0.14 ng/cm^2) on a surface area basis of the air/liquid interface in the lung. Assuming an even deposition of particles, the average distance between the deposited particles will be large enough for the dissolution processes of the scattered particles to be independent

* Corresponding author at: Inhalation Sciences, Hälsovägen 7-9, S-14157 Huddinge, Sweden.
E-mail address: maria.malmlof@inhalation.se (M. Malmlöf).
[1] Address: Rosenhöjdsvägen 26, 152 30 Södertälje, Sweden.

https://doi.org/10.1016/j.ejpb.2019.03.005
Received 8 May 2018; Received in revised form 15 February 2019; Accepted 3 March 2019
Available online 09 March 2019
0939-6411/

of each other [5].

In contrast, in current *in vitro* methods used for testing dissolution/absorption of inhalables, particles are most often deposited in much higher surface concentrations than in the real lung [6–14]. Moreover, the particle deposition methods used also varies between the published methods: Particles are deposited by manually spreading by hand [13]; by even distribution of aerosol over the test surface using aerosol generators such as the PreciseInhale system [11]; or, with the help of either an Andersen cascade impactor (ACI) [6,7,9,12] or a Next Generation Impactor (NGI) [9,10,14] in an attempt to size-classify the particles before deposition on the test surfaces.

Besides the air interface density of particle deposition, primarily determined by the dose [5], there are a several more factors affecting the overall drug dissolution- and absorption of particulate drugs in the lungs: (I) particle size [15] or load of solute in a carrier particle [16]; (II) thickness of the air/blood barrier primarily controlled by region of deposition [17]; (III) the solubility of the solute in the lining layer liquid and tissues [1]. A major complexity in investigating these factors in the lung *in vivo* is the strong covariance between several of the listed parameters, for example between particle size and air/blood barrier thickness. Smaller particles, while dissolving more rapidly, also penetrate deeper in the lung reaching thinner more rapidly traversed barriers during typical ventilation maneuvers with clinical inhalers. It is therefore our strategy in studying the inhalation PK of inhaled particulate drugs to investigate one or two of the parameters at a time while trying to keep the other ones as constant as possible. In the current study we begin with varying the surface density of particle deposition of three different solubility solutes while trying to keep particle size and barrier thickness as constant as possible. This study will be followed by investigation of the particle size effect of a substance on dissolution- and absorption, while keeping mass density of deposition and the barrier thickness constant. Finally, in addition to these *in vitro* studies, by using regional targeting with so called bolus-breathhold techniques [18] in an *in vivo* model, we will investigate the influence on systemic PK by depositing similar-sized particles in the two major regions of the lungs; bronchi and alveoli.

It is thus known that all *in vitro* dissolution methods face the dilemma of compromising between the minimum dose required for confident quantification, and not using an excessive dose density of particles. In general, it would be expected that, in the case where the particles are not interacting, the dissolution- and absorption rates (ng/s) into a mixed receiver eluate will be proportional to mass deposited (ng). As deposited mass is increased, and interactions occur, the dissolution rate would start to plateau irrespective of added mass. This assumes the perfusate does not saturate. It is poorly understood at what point a too high dose density will generate artefactual particle to particle interactions that may affect the dissolution- and absorption of particulate solutes.

The aim of this study was to investigate in one *in vitro* lung dissolution system, the Dissolv*It*, the manner in which the deposited dose of drug particles per test surface area influences the measured dissolution- and absorption rate.

2. Materials and methods

2.1. Materials

We used the PreciseInhale aerosol generator (Inhalation Sciences Sweden AB, Sweden) to evenly deposit three different dry powder particle aerosols on cover slip test surfaces at different dose densities. Subsequently, the *in vitro* dissolution test system Dissolv*It* [11] (Inhalation Sciences Sweden AB, Sweden) was used to generate simulated *in vitro* pharmacokinetic profiles of the deposited particles to investigate the influence of particle deposition density on *in vitro* simulated lung dissolution- and absorption. The substances investigated were the beta agonist salmeterol (SAL) (water solubility 2.26 μg/mL, logP 4.2), the corticosteroids budesonide (BUD) (water solubility 45.7 μg/mL, logP 1.9), and fluticasone propionate (FP) (water solubility 0.51 μg/mL, logP 3.4) (Circassia, UK) [19]; all three in the form of micronized pure APIs. In addition, comparative data on the sensitivity of lung absorption rate to deposited dose was extracted from an already published study on absorption of the low-soluble corticosteroid fluticasone furoate (FF), following inhalation by the *ex vivo* isolated, ventilated and perfused lung of the rat (IPL) [4].

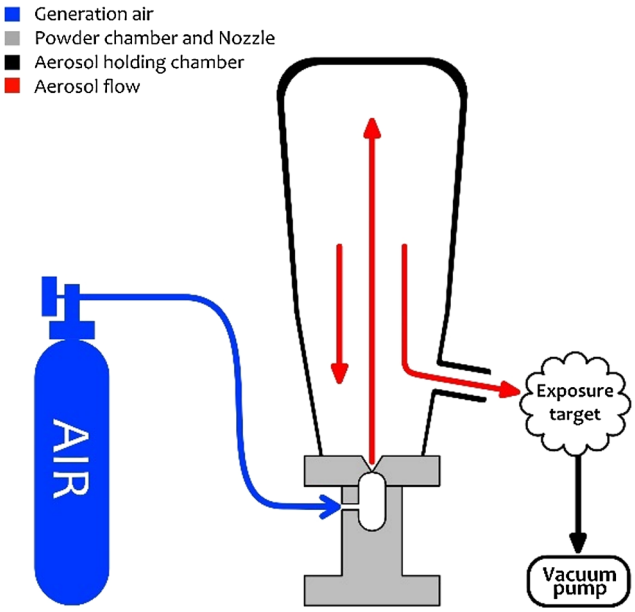

Fig. 1. Schematic picture of PreciseInhale.

2.2. Methods

2.2.1. Aerosol generation

The PreciseInhale [5,20] (Inhalation Sciences, Sweden) aerosol generator was used to generate the test aerosols. Briefly, the DustGun aerosol generator of the PreciseInhale system consists of a powder chamber with an upper, vertical exit nozzle having a diameter of 0.15 mm, a flow registration pneumotach (Fleisch, Switzerland), an aerosol holding chamber, and an exposure line exiting the holding chamber at the base (Fig. 1). The PreciseInhale is connected to a compressed air source for aerosol generation, a vacuum pump for regulating the aerosol flow rate, and a steering computer. In the current study, an aerosol generation pressure of 100 bar and a main valve reset pressure of 40 bar was used. A pre-exposure aerosol mixing period of 0.6 s, and a pressure chamber volume displacement of 7 mm were used. During the aerosol generation procedures, 200–2 mg portions were loaded to the retractable powder chamber bottom, inserted into the PreciseInhale and secured. During the aerosol generation cycle the small volume of air compressed to 100 bar was injected into the powder chamber stirring up the loaded material and ejecting it through the tiny exit nozzle into the holding chamber. After a brief moment the generated aerosol was evenly distributed within the holding chamber and the deposition phase was initiated, at which the generated aerosol was passed over the test surface cover slips using the downstream vacuum pump.

The purpose of aerosol generation procedure was to fully de-agglomerate the micronized API for achieving a well-dispersed aerosol close to the intent of the formulation procedure. We did not try to stay within shear-force levels typical of clinical inhalers, or to choose particle sizes for targeting certain lung regions during clinical ventilation maneuvers.

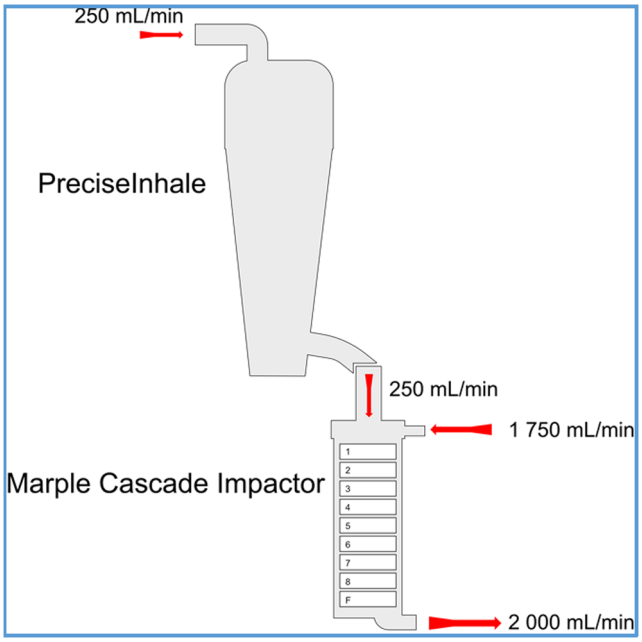

Fig. 2. A flow chart of the PreciseInhale system and the Marple Cascade Impactor used for particle size determination of budesonide.

2.2.2. Particle size determination

For determination of the aerodynamic particle size distribution, a nine-step Marple cascade impactor was used [21]. The aerosol from PreciseInhale entered the cascade impactor directly from the exposure line. The Marple Cascade Impactor is designed to work with a flow rate of 2 L/min. Because the deposition flow rate of the PreciseInhale aerosol deposition chamber was set to 50 mL/min (SAL), 250 mL/min (BUD) and 1000 mL/min (FP) to achieve the target doses, an extra 1950 mL/min (SAL), 1750 mL/min (BUD) and 1000 mL/min (FP) of air was needed to feed the Marple Cascade Impactor with its design volumetric flow rate of aerosol. The additional air was drawn through the inlet of the Marple Cascade Impactor dilution tunnel (Fig. 2).

Following exposures, the drug substance on the impactor stage filters were extracted with methanol and then injected into an HPLC-UV system to determine the amount of substance on each stage. The mass median aerodynamic diameter MMAD (experiments run in triplicate) was calculated as the D_{50} in the cumulative graph.

2.2.3. Deposition of dry powder particles

For the dissolution testing in Dissolv*It*, particles to be tested were deposited on circular glass cover slips (13 mm in diameter, thickness #2, Menzelgläser, Germany) by using the PreciseInhale platform. A specially designed holding chamber for glass coating was used. Nine glasses were placed at the bottom of the aerosol holding chamber, and a mask with nine holes 11 mm in diameter was applied covering the outer perimeter of each glass cover slip, providing an area for test particles to deposit of 0.95 cm^2 on each cover slip. The masking is necessary to ensure that all particles deposited on the cover slip will be available for the dissolution test.

2.2.4. HPLC analysis for dose estimation

To deposit different aerosol doses on the cover slips, different number of powder reloads in PreciseInhale were needed. Both the powder loading amount and the aerosol flow rate for deposition were altered. Less flow and higher amount loaded tended to generate particles of slightly larger aerodynamic size. However, the presented size distributions are based on the lowest aerosol displacement flow rate and maximum load in all cases except for the highest dose of FP. After each completed dose deposition procedure, three representative cover slip glasses were used for the HPLC-UV dose estimation. Prior to the sample analyses, each cover slip sample was dissolved/extracted in the mobile phase. The HPLC analyses were run on a reversed-phase column (Agilent Eclipse XDB-C18, 5 µm, 4.6 × 250 mm) and a PDA-detector (Perkin-Elmer Altus A-10) at a detection wavelength optimized for the API. To create the calibration curve, three portions of API were weighed and diluted in three separate mobile phase solutions. The mobile phase was methanol diluted in water and a stepwise dilution procedure was

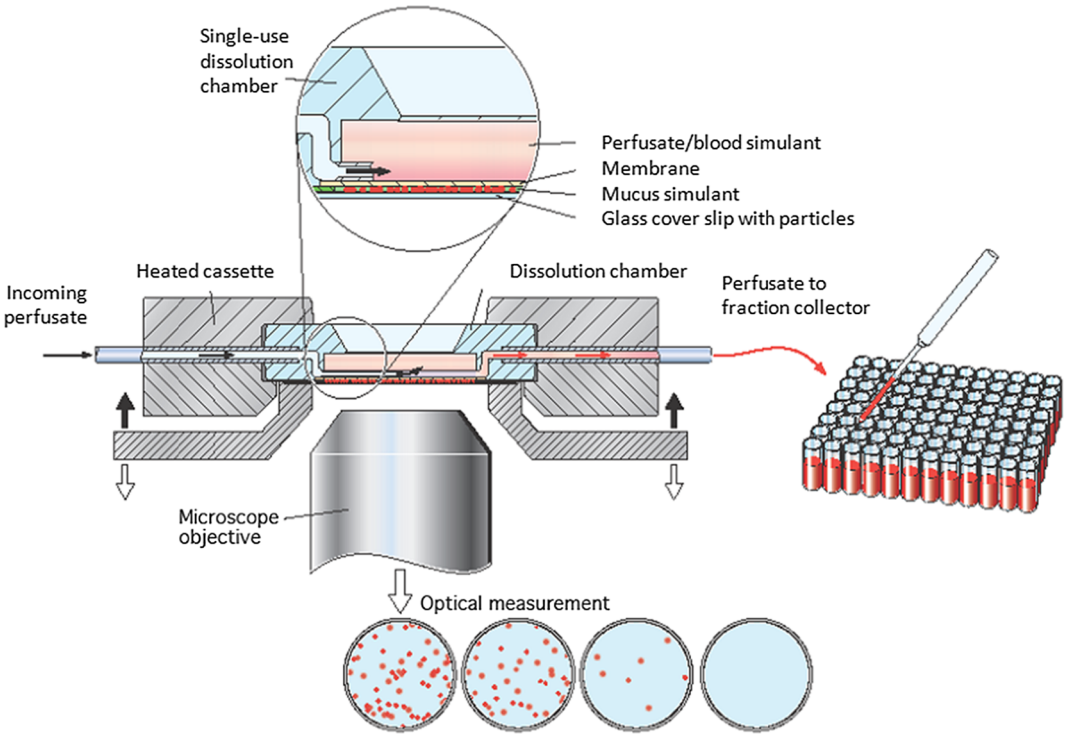

Fig. 3. Schematic picture of the Dissolv*It* set up.

employed to cover the required concentration range.

2.2.5. DissolvIt experiments

Dissolv*It* (Inhalation Sciences, Sweden) is an *in vitro* dissolution method developed to simulate the dissolution- and absorption of dry powder solutes in the lung (Fig. 3) [11].

Briefly, one glass cover slip with deposited particles is placed in a circular holder, particles facing upwards. At experimental start, the particles are automatically contacted with the downward facing mucus simulant coated onto the Dissolv*It* dissolution test chamber. The dissolution chamber consists of (from bottom to top) a thin layer (50 µm) of mucus simulant (1.5% (w/w) polyethylene oxide (Mw = 5000 kDa, SigmaAldrich) in phosphate buffer including 0.4% (w/v) L-alpha phosphatidyl choline (SigmaAldrich) applied on a circular polycarbonate membrane (pore size 0.03 µm, Sterlitech) with a diameter of 12 mm and 10 µm thickness. This membrane is welded onto a molded plastic detail (Euroform, Sweden). In the gap between the hydrophilic polycarbonate membrane (mimicking the basal membrane of the epithelial cells in the airways) and the plastic detail, there is a small void volume of 28 µL, through which a perfusate (4% (w/v) BSA (Santa Cruz Biotechnology, USA) in phosphate buffer, pH 7.4, (mimicking the blood) is pumped at a flow rate of 0.4 mL/min. The whole system is heated to 37 °C.

Solute from the particles dissolving in the mucus simulant then diffuses into the receiver perfusate passing the membrane. The particles are observed in an inverse microscope throughout the dissolution experiment. Photos are taken regularly, and dissolution is manifested as particle disappearance. Complementary, substance absorption is measured by sampling perfusate fractions over time, then analyzed by HPLC-MS/MS (performed by pharm-analyt, Austria). A mass balance is calculated by quantitating the amount undissolved and/or unabsorbed substance left in the system (M_{system}) at the experimental end also using HPLC-MS/MS (pharm-analyt, Austria).

Dissolv*It* experiments were performed in triplicate for each dose and drug substance. The perfusate sampling schedule (Table 1) were designed based on previous experience with the tested drug substances. The samples were collected during 20 s for the first more frequently collected samples of SAL and BUD, or during one min for the remaining samples.

2.2.6. HPLC-MS/MS analysis

An API 6500 QTRAP MS/MS system (AB Sciex, USA) with a Shimadzu HPLC-system was used. All three analytes were separated on a Luna C18-column (50 × 2 mm) in two different analytical runs. Detection was APCI in positive mode for FP and SAL. Detection was APCI in negative mode for BUD.

Calibration ranges were 100 pg/mL to 100 ng/mL for SAL, 50 pg/mL to 50 ng/mL for BUD, 50 pg/mL to 50 ng/mL for FP (Fig. 4). Twenty µL of perfusate was used per sample. This means the absolute levels injected at LLOQ were about one pg for SAL, BUD and FP. Isotopically labelled internal standards were used.

Table 1
Sampling schedule for perfusate samples collected during the Dissolv*It* experiments. The time points specified are the mid values for each sampling interval. The samples were collected for 20–60 s each.

Sample number	SAL (min)	BUD (min)	FP (min)
1	0.33 (20 s)	0.33 (20 s)	4
2	0.67 (40 s)	0.67 (40 s)	8
3	1	1	15
4	1.33 (1 min 20 s)	2	20
5	1.67 (1 min 40 s)	3	30
6	2	5	45
7	3	8	60
8	5	15	120
9	8	30	240
10	15	60	n.a.
11	30	120	n.a.
12	60	n.a.	n.a.

Budesonide was analyzed using a Luna C18 [2], 2 × 50 mm, 5 µm (phenomenex, USA) RP HPLC column on a Shimadzu System. 0.1% acetic acid in water was used as mobile phase A; 0.1% acetic acid in methanol was used as mobile phase B, respectively. A total flow of 0.9 mL/min and a column temperature of 50 °C were applied. The gradient profile was: 0.0–1.8 min: 30% B – > 90% B; 1.8–2.3 min: isocratic flow 90% B; 2.3–3.3 min isocratic flow 30% B. The retention time of Budesonide and its isotopically labelled internal standard (D8-Budesonide) was 1.7 min.

Salmeterol and Fluticasone Propionate were analyzed in one run using an ACE 3AQ, 2.1 × 50 mm, 3 µm (ACE, UK) RP HPLC column on a Shimadzu System. 0.1% acetic acid in water was used as mobile phase A; 0.1% acetic acid in methanol was used as mobile phase B, respectively. A total flow of 0.5 mL/min and a column temperature of 50 °C were applied. The gradient profile was: 0.0–0.5 min: isocratic flow 0% B; 0.5–4.0 min: 40% B – > 100% B; 4.0–5.0 min: isocratic flow 100% B; 5.0–7.0 min: isocratic flow 0% B. The retention time of Salmeterol and its isotopically labelled internal standard (D3-Salmeterol) was 1.3 min; the retention time of Fluticasone Propionate and its isotopically labelled internal standard (D5- Fluticasone Propionate) was 2.0 min, respectively.

2.2.7. Sem

One of the glass cover slips from the same particle deposition procedure intended for the Dissolv*It* experiments was mounted on an aluminium stub and was sputter coated with 10 nm Platinum (Q150T ES, West Sussex, UK). The specimens were analyzed in an Ultra 55 field emission scanning electron microscope (Zeiss, Oberkochen, Germany) at 5 kV using the secondary electron detector. This was done to obtain an overview of particle deposition evenness as well as a detailed indication on the physical state and agglomeration patterns of the three different drug substances.

2.2.8. Data analysis

The analysis generated concentration values in the perfusate (C_{perf}, ng/mL) at all different time points as well as mass values for the undissolved/unabsorbed amount left in Dissolv*It*. The fraction of substance retained in the system either remained undissolved on the glass cover slip or unabsorbed within the mucus simulant (M_{system}).

The perfusate concentration values were used to calculate the cumulative mass found in the perfusate (M_{perf}, ng) according to:

$$M_{perf} = \sum_{i=1}^{n} Q_{perf} \times (t_i - t_{i-1}) \times \left(\frac{C_{perf\,(i)} + C_{perf\,(i-1)}}{2} \right) \quad (1)$$

M_{perf} = cumulatively amount mass (ng) in perfusate
n = number of collected perfusate samples within an experiment
Q_{perf} = volumetric flow rate of perfusate (0.4 mL/min)
t_i = mid time point (min) in sampling interval for sample i
$C_{perf\,(i)}$ = concentration of mass in perfusate sample i (ng/mL)

The mass balance was then calculated for each individual glass cover slip through:

$$M_{dep} = M_{perf} + M_{system} \quad (2)$$

M_{dep} = deposited amount substance on the glass cover slip (ng)
M_{system} = remaining amount undissolved and unabsorbed substance measured in Dissolv*It* at the end of experiment

To investigate actual dose dependence in concentration profiles, the concentration values were normalized to the initial substance mass on

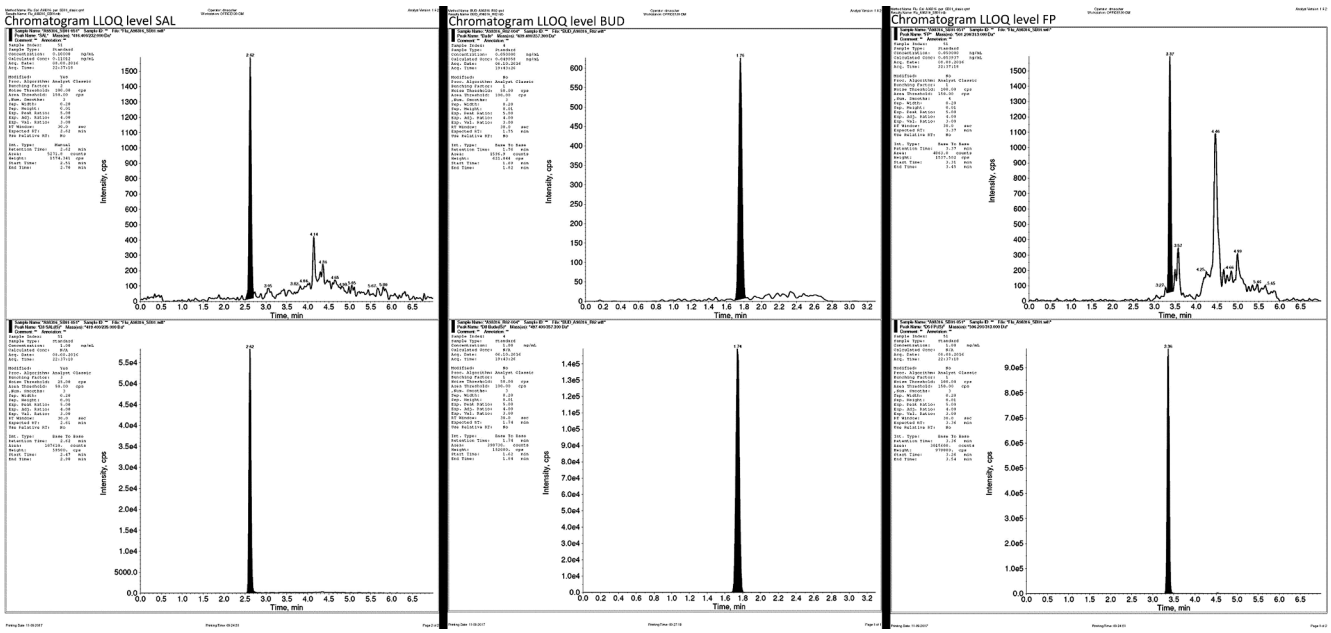

Fig. 4. LLOQ chromatograms for salmeterol (SAL), budesonide (BUD) and fluticasone propionate (FP).

Table 2
Actual deposited doses on the glass cover slips as determined by the mass balance procedure following each experiment are shown in the Actual dose column. The Estimated values show the amounts determined by solvent extraction and HPLC-UV analysis of three test cover slips from each of the aerosol coating procedure.

	SAL (μg/glass)		BUD (μg/glass)		FP (μg/glass)	
	Estimated	Actual	Estimated	Actual	Estimated	Actual
Dose 1	0.20 ± 0.01	**0.23 ± 0.06**	0.26 ± 0.01	**0.27 ± 0.04**	0.27 ± 0.03	**0.22 ± 0.02**
Dose 2	0.76 ± 0.06	**0.68 ± 0.05**	0.82 ± 0.06	**0.85 ± 0.07**	0.85 ± 0.06	**0.79 ± 0.08**
Dose 3	0.97 ± 0.06	**0.95 ± 0.08**	0.97 ± 0.08	**0.96 ± 0.18**	1.00 ± 0.11	**0.88 ± 0.10**
Dose 4	1.55 ± 0.14	**1.59 ± 0.05**	1.51 ± 0.04	**1.64 ± 0.20**	1.65 ± 0.11	**1.31 ± 0.06**
Dose 5	34 ± 4	**27 ± 2**	31 ± 0.3	**11 ± 0.1**	25 ± 5	**28 ± 5**

the glass, expressed as percentage of the deposited dose dissolved per mL of perfusate:

$$C_{norm} = \frac{C_{perf}}{M_{dep}} \times 100 \quad (3)$$

C_{norm} = normalized concentration in the perfusate/% of M_{dep} dissolved/mL perfusate

Normalized cumulative dissolution profiles are also obtained:

$$Frac_{cleared} = \frac{M_c}{M_{dep}} \quad (4)$$

$$Frac_{ret} = 1 - Frac_{cleared} \quad (5)$$

$Frac_{cleared}$ = fraction of M_{dep} that is dissolved and cleared at a given time point
M_c = cumulative mass found in the perfusate at a given time point
$Frac_{ret}$ = retained fraction of M_{dep} undissolved and unabsorbed at a given time point

3. Results

Five different doses ranging from 220 ng to 28 μg of either SAL, BUD or FP were deposited on glass cover slips using the PreciseInhale system. Both the estimated doses (HPLC) and the actual doses (mass balance) are shown in Table 2.

Table 3
The doses on the cover slip glasses (SAL, BUD and FP) expressed as μg/cm^2 and the IPL dose of FF expressed in the same manner.

Dissolv*It*	SAL (μg/cm^2)	BUD (μg/cm^2)	FP (μg/cm^2)	IPL	FF (μg/cm^2)
Dose 1	0.24	0.28	0.23	Low dose	0.00056
Dose 2	0.72	0.89	0.83	High dose	0.0046
Dose 3	1.00	1.01	0.93		
Dose 4	1.67	1.73	1.38		
Dose 5	28	12	29		

In Table 3 the actual doses/glass are recalculated to doses/cm^2. The FF column shows the comparative *ex vivo* deposition on a surface area basis as calculated from the IPL exposures, assuming an approximate area of the rat lung of 1 m^2.

The aerosols generated from the drug substances used in this study were all aerodynamically fine (Table 4).

Fig. 5A show the deposited test aerosols from dose 3 (1.00 μg SAL/cm^2, 1.01 μg BUD/cm^2 and 0.93 μg FP/cm^2) as depicted by SEM. The different substances exhibit different states of agglomeration. In Fig. 5B are shown the particle deposition densities of three different FP doses; dose 1 (0.23 μg/cm^2), dose 2 (0.83 μg/cm^2) and dose 5 (29 μg/cm^2).

FP forms the largest agglomerates. However, most agglomerates formed are chain agglomerates which implies that their aerodynamic diameter remains small, as confirmed by the cascade impactor size distributions (Table 4).

Table 4
The mass median aerodynamic diameter (MMAD) and the geometric standard deviation (GSD) for SAL, BUD and FP.

Formulation	MMAD (μm)	GSD, mean
SAL	1.33	2.50
BUD	1.59	1.98
FP	1.48	2.04

The concentration of the test substances in perfusate- and system wash samples were quantitated using HPLC-MS/MS. The data is presented in different graphs for SAL (Fig. 6), BUD (Fig. 7) and FP (Fig. 8). The absolute concentration data is shown in panels A (SAL, BUD, FP) and B (SAL and BUD), while concentrations normalized to the deposited dose are shown in panels B (FP) and C (SAL and BUD).

From the graphs in Figs. 6–8, pharmacokinetic parameters of the tested drug substances were either extracted or calculated. T_{max} is the time point at which the concentration maximum (C_{max}) as well as the normalized concentration maximum in the perfusate was reached (normalized C_{max}). M_{perf} is the total amount drug substance found in the perfusate over the experimental period. M_{system} is the amount undissolved/unabsorbed drug substance retained in Dissolv*It* at the end of the dissolution experiment. M_{dep} is the total amount drug substance deposited on the glass cover slips as determined from the mass balance (M_{perf} + M_{system}). $Fraction_{ret}$ (graphs found in Figs. 6D (SAL), 7D (BUD) and 8C (FP) is the fraction of the deposited amount of drug substance retained in DissolvIt at the end of experiment (M_{system}/M_{dep}). The pharmacokinetic values are found in Table 5 (SAL), Table 6 (BUD) and Table 7 (FP) respectively.

In Fig. 9 is shown comparative data from the *ex vivo* IPL of the rat on the systemic absorption rate of FF following aerosol administration with the PreciseInhale system at two different dose levels. The results have been derived from calculations based on already published data [5]. The normalized perfusate concentration graphs are shown following deposition of 5.6 μg and 46 μg FF in the rat lung.

4. Discussion

As a basis for discussing soluble drug dissolution in the lungs it is useful to outline the major events involved (Fig. 10). A drug particle has deposited on the airway lining layer of the lungs and begin to dissolve. The liquid concentration of solute reach saturation at the surface of the particle and a dissolution plume is established with concentration gradients into the surrounding liquid medium.

Solute reaching the richly perfused capillary net immediately below the epithelium will be swiftly removed with blood perfusion in what most likely can be viewed as sink conditions. However, this creates a reasonably defined film of more or less stagnant liquid; thicker in the bronchi, thinner in the alveoli. Two parameters are likely to highly influence the dissolution process under these conditions: (I) The average distance between the dissolution plumes surrounding deposited particles in the lungs. Influence of this parameter was a primary purpose of the current investigation. (II) The deposited mass and liquid contact surface area of the portion of solute to be dissolved from each carrier particle/agglomerate creating a local dissolution plume, relative to the solute solubility in this liquid. The latter phenomenon was studied by Ewing et al [16] in the *ex vivo* IPL of the rat for the very low solubility carcinogen benzo(a)pyrene coated onto single-sized particles of amorphous silica over a 1000-fold range of substance load on the carrier particles. The resulting lung absorption kinetics spanned a complete shift from a first-order process where the surrounding plume liquid easily dissolved the local solute load and the absorption proceeded in a sub-saturation process to a zero-order process where the solute in high loads on the carrier particles remained undissolved and saturation prevailed at particle surfaces for prolonged times. This span of kinetic behavior should be similar for most substances with low tissue binding and metabolism on the lipophilic half of the polarity scale.

4.1. Effect of particle deposition density on dissolution ex vivo and in vitro

Before discussing the *in vitro* data obtained with the Dissolv*It*, it is of great value to compare with real lung data derived from exposure to the low-soluble compound, FF, deposited at up to 100-fold the deposition density of a clinically relevant dose [23]. Yet, a 10-fold increase in deposition density of the same micronized drug substance did not affect residence time in the lung at the chosen exposure levels (Fig. 9). The vast majority of the deposited particles was most likely dissolved and absorbed from the rat lung without interference from each other (Fig. 10). This result is also obtained in theoretical models using the

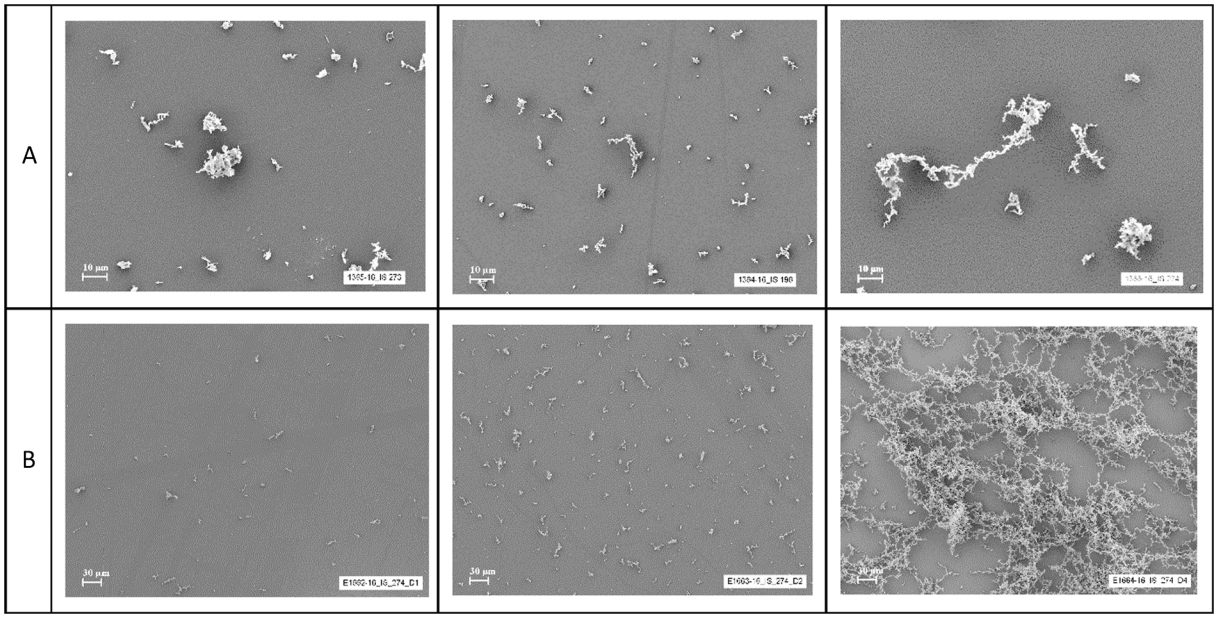

Fig. 5. SEM photos of the investigated materials. (A) Deposition of dose level 3 of (from left to right) SAL (1.00 μg/cm^2), BUD (1.01 μg/cm^2) and FP (0.93 μg/cm^2). (B) The deposition density of FP at different dose levels, from left to right; FP dose 1 (0.23 μg/cm^2), FP dose 2 (0.83 μg/cm^2) and dose 5 (29 μg/cm^2).

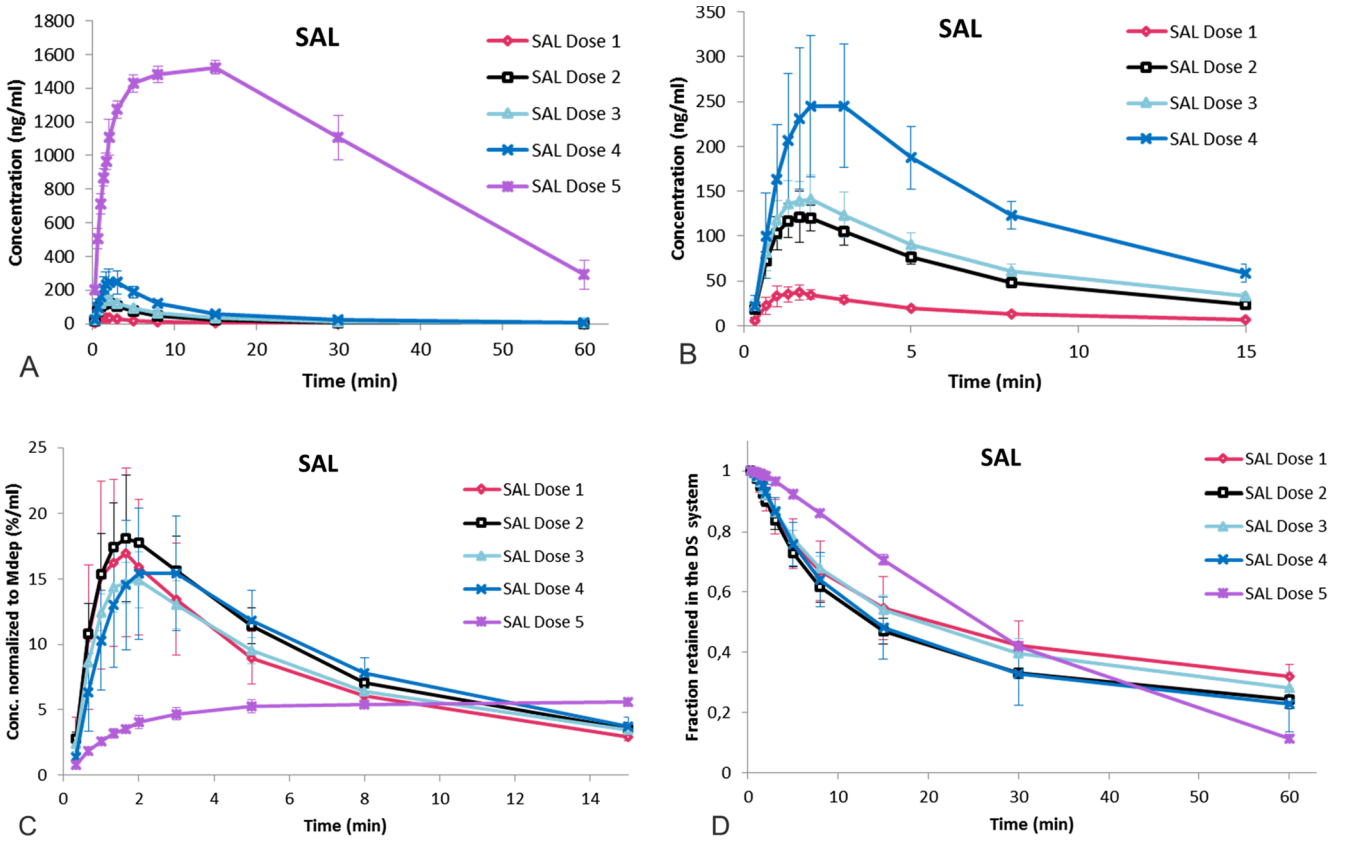

Fig. 6. Dissolution profiles of SAL. (A) The perfusate concentrations of the different SAL doses are shown as a function of time. (B) A close-up of A (minus dose 5) for the first 15 min. (C) c_{norm} of the SAL doses for the first 15 min. (D). $Frac_{retained}$ of the SAL doses is shown as a function of time. The curves are based on mean values of the triplicate experiments and the error bars indicate the standard deviation of the mean.

same assumptions [24].

In contrast, most *in vitro* lung dissolution methods used today have a much smaller dissolution- and absorption surface area available for particle deposition compared to that of the lung. Therefore, we tried to investigate the upper dose limits of one *in vitro* test system, the Dissolv*It*, to find out at what levels increasing deposition densities tend to induce more prominent interference between dissolving particles.

The dose/cm^2 used in Dissolv*It* within this study (230 ng/cm^2 and upwards) is a 1000-fold higher than in the referenced IPL experiments (Table 2). Further, the IPL low dose of 0.6 ng/cm^2 is in the same order of magnitude as the average lung deposition in a human lung following one administration of a typical asthma drug. However, lung deposition will be heterogeneous so probably local doses could be > > 0.6 ng/cm^2 in some zones. For example, at the airway bifurcations in the upper bronchial tree, it is known that local deposition densities of particles may be perhaps a 100-fold higher than the average deposition [25]. Combined with a rapid mucociliary clearance in this region, locally reduced dissolution rates may exist and further contribute to the often observed redistribution of low-solubility drugs from the lungs to the gastro-intestinal tract [26]. The doses used in the current Dissolv*It* study may, thus, still be representative of local lung deposition. The graphs of the normalized dissolution rates also show near independence of dose for the lower masses (e.g. at the 200 ng end), except for FP. This confirms that the system represents a behavior where particles at large are dissolving independently of each other, with no obvious issues regarding limiting perfusate solubilities.

For all three substances tested in Dissolv*It*, higher dose gave as expected higher c_{max} values (Figs. 6A and B, 7A and B, 8A and Tables 5–7), which also correlate with data from the *ex vivo* rat lung [5]. For the t_{max} values there is a weak trend toward increasing values with higher doses for SAL and FP, but not for BUD.

To better illustrate whether the increasing dose densities affected the dissolution/absorption driven residence times, the concentration values at each time point were normalized against the deposited dose. Coinciding curves in such a case indicate that the dissolution-driven retention is independent of the dose density. It is obvious (Figs. 6C, 7C and 8B) that there was a dose effect of dissolution for all substances and the dose dependence increased with decreasing solubility of substances. For SAL the normalized C_{max} is fairly constant for the doses 1–4 implying particles are not interacting. Dose 5 is showing signs of early dissolution limitation due to particle-particle proximity and/or perfusate saturation, however, still showing slightly increasing fractional clearance at one hour compared to doses 1–4 (Fig. 6C).

BUD is showing more dose related dissolution rate limitations than SAL. The highest dose (11 μg) clearly affected dissolution rate. Dose level 4 of BUD may indicate a deviation from the three lowest doses (Fig. 7C). For FP (Fig. 8B) the dissolution-driven retention is dependent on the dose over the range tested. The dissolution is there completely limited by the system, and deposition of the same test doses on the glasses are important for comparison of different formulations.

Complementary to the normalized concentration graphs, the fraction retained graphs (Figs. 6D, 7D and 8C) are also indicative of the dose effect on the dissolution and absorption pharmacokinetics. The fraction retained is the amount of drug remaining undissolved and not absorbed into perfusate as a function of time in relation to the initially deposited dose. Also listed in Tables 5–7 are the fractions retained at the end of the perfusate sampling periods.

In the current *in vitro* dissolution system, there seems to be a certain limit in the density of particle deposition above which increasing doses will cause a distinctive increase in drug retention. This sensitivity to deposition density increases markedly with decreasing solubility of the test substance. The reason for increasing model barrier retention with

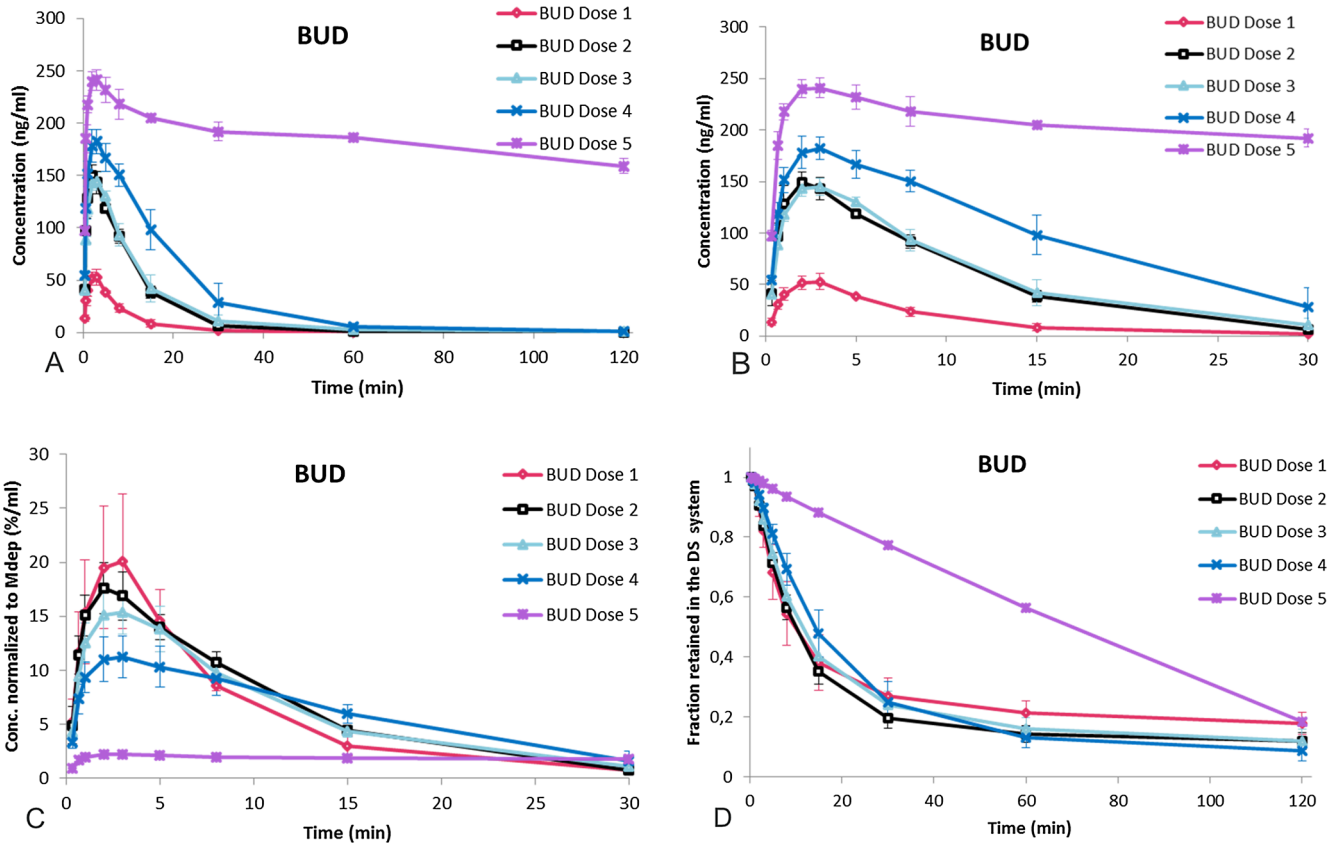

Fig. 7. Dissolution profiles of BUD. (A) The concentration in the perfusate of the different BUD doses is shown as a function of time. (B) A close-up of A during the first 30 min. (C) c_{norm} for the BUD doses during the first 30 min. (D) $Frac_{ret}$ is shown for the different BUD doses as a function of time. The curves are based on mean values of the triplicate experiments and the error bars indicate the standard deviation of the mean.

deposition density is most likely the increasing dissolution interference between the deposited particles as depicted in Fig. 10. The increasing retention sensitivity with decreasing substance solubility is linked to the increasing volumes of receptor fluid of the model barrier needed to dissolve the test particles. This is well illustrated by the shift in correlation between applied dose and detected C_{max} of the same substance. If the applied dose has no influence on drug retention there would be a close to 100% correlation between dose and C_{max} over an increasing dose interval, which is the case for FF in the *ex vivo* single-pass perfusate of the IPL (Fig. 9). For the more soluble drug SAL over a 100-fold dose increase in the Dissolv*It,* the C_{max} fell to 35% of its expected value (Table 5), whereas as this correlation fell to only 1.6% for the low-soluble FP (Table 7).

It is obvious that aerosol agglomeration accompanies all dissolution test methods involving aerosol capture followed by a dissolution procedure, the current as well as others. However, aerosol agglomeration is also an important companion of inhalation exposures. Its influence on aerodynamics as well as dissolution kinetics is closely linked to the nature of the agglomerates. Globular clusters never deagglomerated during aerosolization, have aerodynamic diameters close to their geometric diameters, so both aerodynamic- and dissolution properties will change rapidly with increasing degree of agglomeration. In contrast, when agglomeration occurs post-generation in the produced aerosol, most of the agglomerates formed are chain agglomerates with quite high aspect ratios. Such agglomerates increase both their aerodynamic diameters and dissolution times much more gradual with increasing degree of agglomeration. Chain agglomerates are a significant feature when the high power DustGun generator is employed to produce the concentrated aerosols used in the current study [27].

In evaluating the currently derived data set from the Dissolv*It*, it is important to identify how the two major design features of the dissolution set up affect performance: I) The study particles can either be separated from the streaming receptor fluid (perfusate) by a defined diffusional barrier (flow past), or the streaming receptor fluid may surround the study particles (flow through). II) The receptor fluid can be supplied in either single-pass, dynamic mode, or from a fixed volume in mixed contact with the dissolving particles; static mode. These design choices have a profound influence on the method characteristics. The defined barrier is more similar to the *in vivo* situation where sink conditions are more likely to be located at the barrier-perfusate contact surface. The barrier residence time of dissolving particles will likely be more insensitive to perfusate flow rate or stirring speed. In contrast, during flow through perfusion in a filter cassette or in a stirred particle suspension, the dissolving particles will be surrounded by boundary layer films whose thickness will be dependent on the local flow rate or stirring speed [28]. The residence time will decrease with increasing flow rate [7]. While such a phenomenon is likely to be much less pronounced during *in vivo* exposures, it may provide the flow through method design with a greater resilience to interference dissolution, particularly at higher perfusate flow rates with thinner boundary layer films, this will, however, be at the price of much less *in vivo*-like characteristics.

Preceding the dissolution methods is the equally important choice of method to deposit the investigated aerosol on the various test surfaces used. Three major deposition methods can be identified: (1) **Airway-like deposition** has been used so far in the current study and even more realistically in recent studies [29]. The investigated aerosol slides over the test surface creating a rather mild impaction and sedimentation of particles, that are likely to have a slightly larger size distribution than the exiting aerosol. It is possible that the efficiency during airway-like

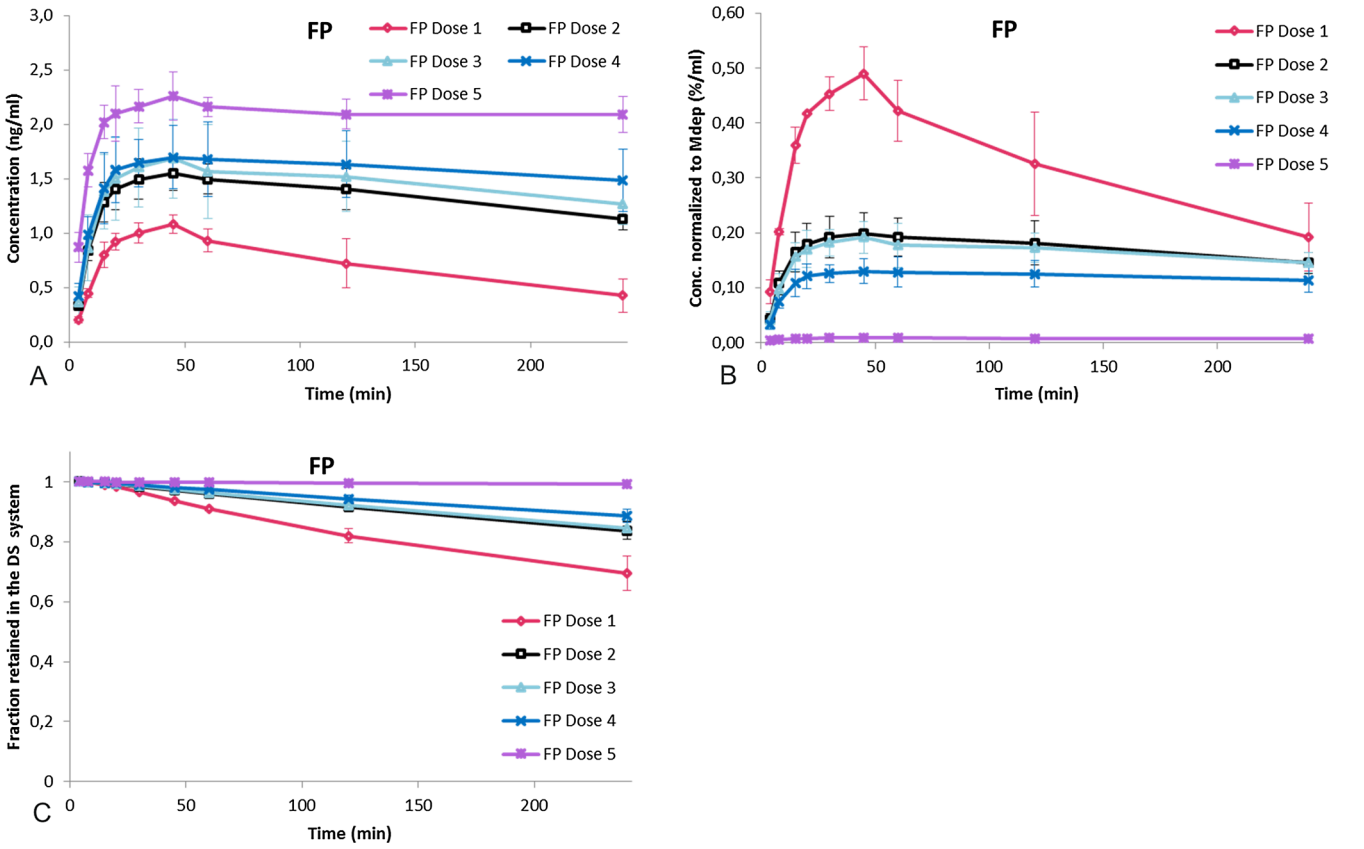

Fig. 8. Dissolution profiles of FP. (A) The concentration in the perfusate of the different FP doses is shown as a function of time. (B) c_{norm} for the FP doses. (C) $Frac_{ret}$ of the FP doses as a function of time. The curves are based on mean values of the triplicate experiments and the error bars indicate the standard deviation of the mean.

deposition will be changed during increasing already existing deposition densities on the test surface. (2) **Total deposition** of aerosol can be accomplished either by complete sedimentation [30] or by total filter capture [7]. During total sedimentation, it is likely that re-agglomeration of aerosol particles will occur before deposition, potentially changing dissolution properties. Filter capture can probably maintain size distribution of deposited aerosol closer to airborne particles better than the other methods. However, the particles will be deposited on a porous filter surface that has a very large sorptive surface that may significantly affect the detected dissolution process. Finally, (3) **Size-fractionated deposition** by placing test surfaces in cascade impactors such as the Next Generation Impactor or the Anderson Cascade Impactor [10]. There is an obvious risk that aggregation and too dense deposition of particles in the impaction zones below the impactor nozzles will cause significantly slower dissolution because of solute plume interference, such as indicated in the current study.

4.2. Validation of DissolvIt

Besides the general findings about dose effects on *in vitro* dissolution, all experiments performed within this work contribute to further validation of Dissolv*It*. The estimated dose values (measured by HPLC) and the actual dose values (from mass balance) are quite close in all cases except for the highest BUD dose (Table 1). This indicates that our HPLC dose estimation method is reliable as corroborated by the mass balance [11]. One possible explanation for the unreliable dose prediction for high doses could be that the particle deposition is more dependent on the already deposited material than at low doses. A further advantage of using PreciseInhale for the aerosol generation and dose deposition is the low RSD accomplished, also at low doses; in the range of 9–26% variation at doses around 220 ng/glass cover slip (Table 2).

Comparing the pharmacokinetic profiles (Figs. 6–8), it can be concluded that the dose affects particle dissolution (Figs. 6C, 7C and 8B) and that the spontaneously occurring variations in dose deposition of the PreciseInhale system produce a corresponding variability in the generated non-normalized raw output data, such as $C_{max,}$ that is "acceptable". For SAL, the results are similar for dose 2 (0.68 μg/glass cover slip) and dose 3 (0.95 μg/glass cover slip), which corresponds to a RSD tolerance of 40%. The same figures for BUD is dose 2 (0.85 μg/glass cover slip) and dose 3 (0.96 μg/glass cover slip) which gives a tolerance in RSD of at least 13%. For FP, it is dose 2 (0.79 μg/glass cover slip) and dose 3 (0.88 μg/glass cover slip) which results in a RSD tolerance of 11%. The different doses tested were chosen with the aim of covering a wide concentration range, and to obtain most doses close to what earlier have been used in Dissolv*It* (around 1 μg/glass cover slip [11]), and also to have two doses quite close to investigat acceptable RSDs. We found that in all our cases dose 2 and dose 3 could be classified as quite similar and that a RSD of < 11% between repeated doses for dissolution testing seems acceptable. This may also suggest that the deposited dose density used in Dissolv*It* should not exceed 1 μg/glass cover slip as well as /cm^2, and maybe even lower for low soluble substances.

4.3. How to best simulate lung dissolution in vitro?

There are a number of different *in vitro* dissolution methods used today [6–14] to investigate the dissolution properties of inhaled powder drug substances. Two main purposes are at hand; (1) as a quality control method to ascertain that the dissolution properties of different batches of manufactured drug substances remain within specified quality criteria, and (2), as an *in vitro* tool for predicting the *in vivo* dissolution- and absorption behavior of an inhaled powder drug

Table 5
SAL pharmacokinetic parameters.

Exposure material	t_{max} (min)	C_{max} (ng/ml)	Normalized C_{max} (%/ml)	Mass balance			$Fraction_{ret}$
				M_{perf} (ng)	M_{system} (ng)	M_{dep} (ng)	
SAL Dose 1	1.7 ± 0.3	37 ± 8	17 ± 6	156 ± 31	75 ± 27	232 ± 57	0.32 ± 0.04
SAL Dose 2	1.8 ± 0.2	127 ± 20	19 ± 4	513 ± 39	164 ± 26	677 ± 50	0.24 ± 0.03
SAL Dose 3	1.9 ± 0.2	166 ± 143	15 ± 2	681 ± 92	264 ± 41	945 ± 76	0.28 ± 0.05
SAL Dose 4	2.3 ± 0.6	249 ± 73	16 ± 5	1224 ± 119	366 ± 159	1591 ± 46	0.23 ± 0.09
SAL Dose 5	12 ± 6	1525 ± 41	5.6 ± 0.2	24286 ± 1857	3109 ± 324	27395 ± 1840	0.11 ± 0.01

Table 6
BUD pharmacokinetic parameters.

Exposure material	t_{max} (min)	C_{max} (ng/ml)	Normalized C_{max} (%/ml)	Mass balance			$Fraction_{ret}$
				M_{perf} (ng)	M_{system} (ng)	M_{dep} (ng)	
BUD Dose 1	2.7 ± 0.6	53 ± 7	20 ± 6	222 ± 26	50 ± 17	271 ± 42	0.18 ± 0.04
BUD Dose 2	2.0 ± 0.0	149 ± 10	18 ± 2	751 ± 38	103 ± 32	854 ± 69	0.12 ± 0.03
BUD Dose 3	2.7 ± 0.6	145 ± 9	15 ± 2	847 ± 176	112 ± 35	958 ± 176	0.12 ± 0.04
BUD Dose 4	2.7 ± 0.6	183 ± 13	11 ± 2	1504 ± 237	139 ± 45	1643 ± 203	0.09 ± 0.04
BUD Dose 5	2.3 ± 0.6	241 ± 10	2.2 ± 0.1	8882 ± 94	2003 ± 69	10885 ± 147	0.18 ± 0.00

Table 7
FP pharmacokinetic parameters.

Exposure material	t_{max} (min)	C_{max} (ng/ml)	Normalized C_{max} (%/ml)	Mass balance			$Fraction_{ret}$
				M_{perf} (ng)	M_{system} (ng)	M_{dep} (ng)	
FP Dose 1	45 ± 0	1.1 ± 0.1	0.49 ± 0.05	68 ± 14	154 ± 20	222 ± 19	0.70 ± 0.06
FP Dose 2	45 ± 0	1.6 ± 0.2	0.20 ± 0.04	126 ± 11	662 ± 91	788 ± 80	0.84 ± 0.03
FP Dose 3	40 ± 9	1.7 ± 0.4	0.19 ± 0.03	137 ± 29	740 ± 76	876 ± 96	0.84 ± 0.02
FP Dose 4	45 ± 15	1.7 ± 0.3	0.13 ± 0.02	149 ± 28	1159 ± 67	1308 ± 58	0.89 ± 0.02
FP Dose 5	110 ± 1-13	2.3 ± 0.2	0.01 ± 0.00	198 ± 10	27490 ± 5-266	27617 ± 5276	0.99 ± 0.00

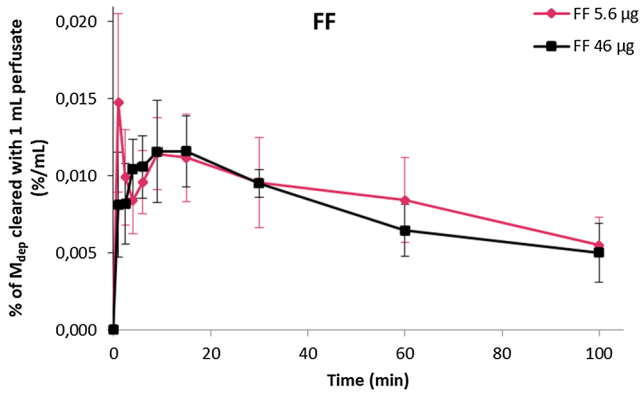

Fig. 9. Percent of the initially deposited FF dose cleared per mL single-pass perfusate over time in the IPL (%M_{DEP}/mL). Based on data from Ref. (5).

substance (IVIVC). The latter purpose clearly being more of a challenge, and where there is no common conclusion on which *in vitro* method simulates reality best [12,13]. Neither is there any general recommendations or defined standard methods stated by legal bodies like FDA, regarding dissolution testing of inhalable pharmaceuticals [31]. However, it is a desired goal to find methods that provide better *in vitro-in vivo* correlations.

In the real lung (rodents, dogs, monkeys as well as in humans), the surface area is always very large compared to the deposited dose of inhalable drugs. This means that distance between deposited particles is most often long enough for not influencing the dissolution of each other. This deposition density *in vivo* is very difficult to simulate *in vitro*, which will be an issue during all *in vitro* lung dissolution studies. In doing so it is important to understand what compromises can be done and what effects this may have and when such effects can be accommodated or not. The dose density and distance between particles must be carefully considered, and we have shown that the highest doses used (11–28 µg/glass cover slip) profoundly affects the dissolution profiles obtained. However, by using lower doses with an RSD between repeated doses below 10–15%, consistent output data are produced that can be used to compare different preparations of the same compound.

5. Conclusion

In this study we have shown that the deposition density of a tested substance in an *in vitro* lung dissolution test system will influence the resulting dissolution-driven residence time, whereas no such dose-related effect was seen in the *ex vivo* rat lung. This needs to be considered when trying to simulate *in vitro* the dissolution and absorption of drugs in the lung. Control of the deposited dose on the *in vitro* test surface with good repeatability is one important parameter to consider. Further cross-validation with *ex vivo-in vivo* lung PK data using substantially similar deposited aerosols is also important for increasing the understanding and usefulness of *in vitro* dissolution methods.

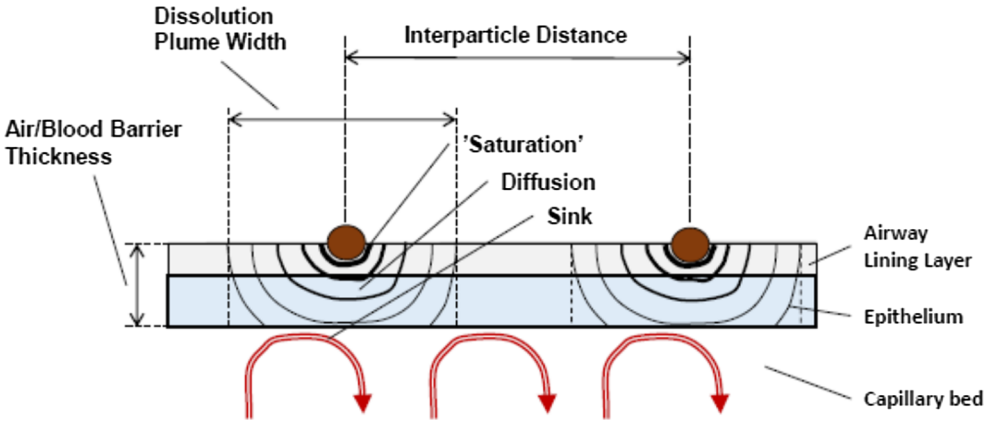

Fig. 10. A schematic of soluble particle dissolution- and absorption following deposition as aerosols on the airway lining layer [22].

Acknowledgement

Fig. 3 is reproduced with permission from Respiratory Drug Delivery 2014, Virginia Commonwealth University and RDD Online. We would like to thank Kjell Hultenby for taking the SEM photos.

Funding

This research did not receive any specific grant from funding agencies in the public, commercial, or not-for-profit sectors.

Conflicts of interest

Per Gerde, Mattias Nowenwik and Iwona Rådberg are minority shareholders in Inhalation Sciences Sweden AB. Maria Malmlöf, Mattias Nowenwik, Ewa Selg and Per Gerde are employed by Inhalation Sciences Sweden AB.

References

[1] B. Forbes, P. Backman, D. Christopher, M. Dolovich, B.V. Li, B. Morgan, In vitro testing for orally inhaled products: developments in science-based regulatory approaches, AAPS J. 17 (4) (2015) 837–852.
[2] T. Riley, D. Christopher, J. Arp, A. Casazza, A. Colombani, A. Cooper, M. Dey, J. Maas, J. Mitchell, M. Reiners, N. Sigari, T. Tougas, S. Lyapustina, Challenges with developing in vitro dissolution tests for orally inhaled products (OIPs), AAPS PharmSciTech. 13 (3) (2012) 978–989.
[3] S.P. Velaga, J. Djuris, S. Cvijic, S. Rozou, P. Russo, G. Colombo, A. Rossi, Dry powder inhalers: an overview of the in vitro dissolution methodologies and their correlation with the biopharmaceutical aspects of the drug products, Eur. J. Pharm. Sci. 113 (2018) 18–28.
[4] E. Frohlich, G. Bonstingl, A. Hofler, C. Meindl, G. Leitinger, T.R. Pieber, E. Roblegg, Comparison of two in vitro systems to assess cellular effects of nanoparticles-containing aerosols, Toxicol. In Vitro (2012).
[5] E. Selg, P. Ewing, F. Acevedo, C.O. Sjoberg, A. Ryrfeldt, P. Gerde, Dry powder inhalation exposures of the endotracheally intubated rat lung, ex vivo and in vivo: the pulmonary pharmacokinetics of fluticasone furoate, J. Aerosol. Med. Pulm Drug Deliv. 26 (4) (2013) 181–189.
[6] D. Arora, K.A. Shah, M.S. Halquist, M. Sakagami, In vitro aqueous fluid-capacity-limited dissolution testing of respirable aerosol drug particles generated from inhaler products, Pharm. Res. 27 (5) (2010) 786–795.
[7] N.M. Davies, M.R. Feddah, A novel method for assessing dissolution of aerosol inhaler products, Int. J. Pharm. 255 (1–2) (2003) 175–187.
[8] T.J. Franz, Percutaneous absorption on the relevance of in vitro data, J, Invest. Dermatol. 64 (3) (1975) 190–195.
[9] M. Rohrschneider, S. Bhagwat, R. Krampe, V. Michler, J. Breitkreutz, G. Hochhaus, Evaluation of the transwell system for characterization of dissolution behavior of inhalation drugs: effects of membrane and surfactant, Mol. Pharm. 12 (8) (2015) 2618–2624.
[10] Y.J. Son, J.T. McConville, Development of a standardized dissolution test method for inhaled pharmaceutical formulations, Int. J. Pharm. 382 (1–2) (2009) 15–22.
[11] P. Gerde, M. Malmlof, L. Havsborn, C.O. Sjoberg, P. Ewing, S. Eirefelt, K. Ekelund, DissolvIt: an in vitro method for simulating the dissolution and absorption of inhaled dry powder drugs in the lungs, Assay Drug Dev. Technol. 15 (2) (2017) 77–88.
[12] S. May, B. Jensen, M. Wolkenhauer, M. Schneider, C.M. Lehr, Dissolution techniques for in vitro testing of dry powders for inhalation, Pharm. Res. 29 (8) (2012) 2157–2166.
[13] R.O. Salama, D. Traini, H.K. Chan, P.M. Young, Preparation and characterisation of controlled release co-spray dried drug-polymer microparticles for inhalation 2: evaluation of in vitro release profiling methodologies for controlled release respiratory aerosols, Eur. J. Pharm. Biopharm. 70 (1) (2008) 145–152.
[14] Y.-J. Son, M. Horng, M. Copley, J.T. McConville, Optimization of an in vitro dissolution test method for inhalation formulations, Dissolut. Technol. (2010) 6–13.
[15] W.I. Higuchi, E.N. Hiestand, Dissolution rates of finely divided drug powders. I. Effect of a distribution of particle sizes in a diffusion-controlled process, J. Pharm. Sci. 52 (1963) 67–71.
[16] P. Ewing, B. Blomgren, A. Ryrfeldt, P. Gerde, Increasing exposure levels cause an abrupt change in the absorption and metabolism of acutely inhaled benzo(a)pyrene in the isolated, ventilated, and perfused lung of the rat, Toxicol. Sci. 91 (2) (2006) 332–340.
[17] P. Gerde, B.A. Muggenburg, R.F. Henderson, Disposition of polycyclic aromatic hydrocarbons in the respiratory tract of the Beagle dog: III. Mechanisms of the dosimetry, Toxicol. Appl. Pharmacol. 121 (1993) 328–334.
[18] W.D. Bennett, J.S. Brown, K.L. Zeman, S.C. Hu, G. Scheuch, K. Sommerer, Targeting delivery of aerosols to different lung regions, J Aerosol Med. 15 (2) (2002) 179–188.
[19] Unknown. In: PubChem Compound Database: National Center for Biotechnology Information.
[20] E. Selg, F. Acevedo, R. Nybom, B. Blomgren, Å. Ryrfeldt, P. Gerde, Delivering horseradish peroxidase as a respirable powder to the isolated, perfused and ventilated lung of the rat: the pulmonary disposition of an inhaled model biopharmaceutical, J. Aerosol. Med. Pulmonary Drug Deliv. 23 (5) (2010) 273–284.
[21] V.A. Marple, J.E. McCormack, Personal sampling impactor with respirable aerosol penetration characteristics, Am. Ind. Hyg. Assoc. J. 44 (12) (1983) 916–922.
[22] P. Gerde, Aerosol dissolution: Breaking through the in vitro–in vivo barrier, in: Inhalation Asia, Shenyang, China, 2015.
[23] D.I. Bernstein, E.D. Bateman, A. Woodcock, W.T. Toler, R. Forth, L. Jacques, C. Nunn, P.M. O'Byrne, Fluticasone furoate (FF)/vilanterol (100/25 mcg or 200/25 mcg) or FF (100 mcg) in persistent asthma, J. Asthma 52 (10) (2015) 1073–1083.
[24] S. May, B. Jensen, C. Weiler, M. Wolkenhauer, M. Schneider, C.M. Lehr, Dissolution testing of powders for inhalation: influence of particle deposition and modeling of dissolution profiles, Pharm. Res. 31 (11) (2014) 3211–3224.
[25] I. Balásházy, W. Hofmann, T. Heistracher, Computation of local enhancement factors for the quantification of particle deposition patterns in airway bifurcations, J. Aerosol. Sci. 30 (2) (1999) 185–203.
[26] S. Edsbäcker, P. Wollmer, O. Selroos, L. Borgstrom, B. Olsson, J. Ingelf, Do airway clearance mechanisms influence the local and systemic effects of inhaled corticosteroids? Pulm. Pharmacol. Ther. 21 (2) (2008) 247–258.
[27] P. Gerde, P. Ewing, L. Låstbom, J. Waher, G. Lidén, Å. Ryrfeldt, A novel method to aerosolize powder for short inhalation exposures at high concentrations: Isolated rat lungs exposed to respirable diesel soot, Inhalation Toxicol. 16 (1) (2004) 45–52.
[28] A.T. Lu, M.E. Frisella, K.C. Johnson, Dissolution modeling: factors affecting the dissolution rates of polydisperse powders, Pharm. Res. 10 (9) (1993) 1308–1314.
[29] B.K. Huynh, D. Traini, D.R. Farkas, P.W. Longest, M. Hindle, P.M. Young, The development and validation of an in vitro airway model to assess realistic airway deposition and drug permeation behavior of orally inhaled products across synthetic membranes, J. Aerosol. Med. Pulm. Drug Deliv. 31 (2) (2018) 103–108.
[30] S. Hein, M. Bur, U.F. Schaefer, C.M. Lehr, A new Pharmaceutical Aerosol Deposition Device on Cell Cultures (PADDOCC) to evaluate pulmonary drug absorption for metered dose dry powder formulations, Eur. J. Pharm. Biopharm. 77 (1) (2011) 132–138.
[31] A. Fuglsang, The US and EU regulatory landscapes for locally acting generic/hybrid inhalation products intended for treatment of asthma and COPD, J. Aerosol. Med. Pulm Drug Deliv. 25 (4) (2012) 243–247.